# Modern sedimentary dynamics in the Southwestern Atlantic Contouritic Depositional System: New insights from the Uruguayan margin based on a geochemical approach

**Article** *in* Marine Geology · March 2016

DOI: 10.1016/j.margeo.2016.03.008

Paula Franco-Fraguas
Universidad de la República de Uruguay
**19** PUBLICATIONS **184** CITATIONS

Leticia Burone
Universidad de la República de Uruguay
**39** PUBLICATIONS **1,181** CITATIONS

Michel M Mahiques
University of São Paulo
**222** PUBLICATIONS **3,159** CITATIONS

Leonardo Ortega
Ministry of Livestock, Agriculture and Fisheries
**70** PUBLICATIONS **727** CITATIONS

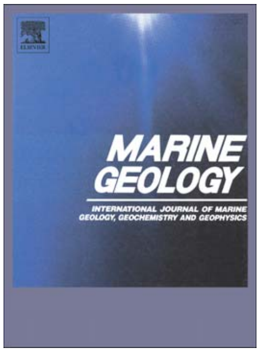

# Modern sedimentary dynamics in the Southwestern Atlantic Contouritic Depositional System: New insights from the Uruguayan margin based on a geochemical approach

Paula Franco-Fraguas, Leticia Burone, Michel Mahiques, Leonardo Ortega, Alvar Carranza

PII: S0025-3227(16)30027-5
DOI: doi: 10.1016/j.margeo.2016.03.008
Reference: MARGO 5428

To appear in: *Marine Geology*

Received date: 5 May 2015
Revised date: 23 February 2016
Accepted date: 15 March 2016

Please cite this article as: Franco-Fraguas, Paula, Burone, Leticia, Mahiques, Michel, Ortega, Leonardo, Carranza, Alvar, Modern sedimentary dynamics in the Southwestern Atlantic Contouritic Depositional System: New insights from the Uruguayan margin based on a geochemical approach, *Marine Geology* (2016), doi: 10.1016/j.margeo.2016.03.008

# Modern sedimentary dynamics in the Southwestern Atlantic Contouritic Depositional System: New insights from the Uruguayan margin based on a geochemical approach

Franco-Fraguas, Paula[a*]; Burone, Leticia[a]; Mahiques, Michel[b]; Ortega, Leonardo[c]; Carranza, Alvar[d].

* (corresponding author) (email: paulafrancof@gmail.com, Tel: +598-2-5258618-21)

[a] Universidad de la República, Facultad de Ciencias, Sección Oceanología. Iguá 4225, Montevideo 11400, Uruguay.

[b] Instituto Oceanográfico da Universidade de São Paulo, Praça do Oceanográfico 191, 05508-120 São Paulo, SP, Brazil.

[c] Dirección Nacional de Recursos Acuáticos, Ministério de Ganadería Agricultura y Pesca. Constituyente 1497, Montevideo, Uruguay.

[d] Universidad de la Republica, Centro Universitario Regional Este-CURE-Sede Maldonado, Uruguay and Área Biodiversidad y Conservación, Museo Nacional de Historia Natural, Montevideo, Uruguay.

## Abstract

Recent high-resolution, multidisciplinary studies have provided models of modern and ancient sedimentary processes along the Uruguayan slope (34°S to 36°S), a strategic location in the Southwestern Atlantic margin (SAM). According to these models, modern surface sedimentation is controlled by the transition between the Subtropical Shelf Front and the Brazil-Malvinas Confluence (BMC), and presumably by the summer Rio de la Plata (RdlP) buoyant plume. Ancient sedimentary dynamics is reflected as the northernmost distribution of the contouritic terraces present in the Argentinean margin, reflecting the position of the BMC during glacial stages. In this work, the spatial correlation of previous evidence from modern (surface facies) and ancient (geomorphological features) sedimentation provides a sound framework in order to interpret novel information on the geochemical composition of surface sediments. Proxies for the origins of lithogenic (Nd, Al/Si, and Fe/K) and organic matter (C/N, $\delta^{13}C$, and $\delta^{15}N$), previously calibrated for the SAM, and the elemental compositions (Al, TI, Fe, K, Mn, Ca, P, Mg, Ba, and Si) of surface sediments were used to test working hypotheses on sediment provenance, surface productivity and the environmental control of elementary composition. The distribution of surface sediments is correlated with regional geomorphology, which includes contouritic terraces in the south and a progradational slope in the north. This supports the idea of a strong morphological control on the modern sedimentary processes. However, the distribution and content of terrigenous, biogenic and erosional elements, together with the dominance of Pampean-Patagonian sediments, suggests that 1) the RdlP does not contribute with any lithogenic sediments to the slope and, instead, fertilizes open waters with contributions consisting of mixed marine organic matter; 2) in the north, the strong action of the BC and the re-circulated AAIW below promotes redistribution of sediments from the shelf and upper slope towards the middle slope, including sandy spillover/slump transport and hemipelagic sedimentation re-suspended from the continental shelf; 3) with respect to glacial stages, this across-slope sedimentation was displaced southwards dominating even the northernmost distribution of contouritic terraces and 4) sedimentation related to contouritic features, as modern depositional and erosional sedimentation, was restricted to the south accompanying the distribution of the MC. Thus, although the core hypothesis of the previous modern sedimentary model can be retained, considerable improvements in our knowledge of the sediment dynamics in the SAM have emerged from the present analysis of geochemical proxies.

**Keywords**: Southwestern Atlantic margin, surface facies, Argentinean Contourite Depositional system, Uruguayan slope, geochemical content, sediment sources

## 1. Introduction

The geochemical composition and distribution of surface marine sediments reflects modern sedimentary processes and can be used to infer past environmental conditions. Source rocks and circulation regimes can be evaluated by analysing long-lived radioisotopes because of the rapid incorporation of river-originated neodymium (Nd) into marine sediments (DePaolo, 1988). Similarly, the analysis of element ratios (i.e., Al/Si and Fe/K) can assist in the identification of the origin of sediments because these ratios reflect the climatic conditions of the continental parent rocks (Weltje and Tjallingii, 2008). The characteristics of the organic matter that is deposited in the superficial sediments of marine regions are widely used in correlative analyses of several oceanographic processes (Müller and Suess, 1979; Stein, 1991; Faganeli et al., 1994; Meyers, 1997). The marine versus terrestrial origins of organic matter can be inferred from stable isotopes of carbon and nitrogen and elemental C/N ratios (Prahl et al., 1994; Mahiques, 1999; Burone et al., 2013). The contents and distributions of minor (Ba) and major (i.e., Si, Ti, Fe, Al, K, Mn, Ca, P, Mg) elements provide additional information regarding marine depositional settings (Martin and Meybeck, 1979 ; Murray et al., 1995; Shumilin et al., 2002; Lim et al., 2006; Yang and Youn, 2007; Burone et al., 2013), including both qualitative and quantitative aspects of biological production and, notably, the mineralogical and textural characteristics of the sediment particles. Thus, the joint analysis of the above mentioned proxies is a key tool for evaluating modern sedimentation processes, allowing both the improvement of paleoceanographic reconstructions and the forecasting of future conditions.

The hydrology of the modern Southwestern Atlantic margin (SAM), which is among the most productive and energetic areas worldwide, is well known at a macro-scale. The system is dominated by the confluence of currents with contrasting thermohaline properties, namely, the southward-flowing Brazil Current (BC), the northward-flowing Malvinas Current (MC), and the outflow of the Rio de la Plata (RdlP), which discharges freshwater from the second largest hydrographic basin in South America (average value of 22,000 $m^3/s$; Framiñan and Brown, 1996). This confluence occurs in the Brazil–Malvinas Confluence zone (BMC) in the open ocean (Olson et al., 1988) and extends towards the Subtropical Shelf Front (STSF) on the continental shelf (Piola et al., 2008). This hydrological system accounts for most of the modern sedimentation at regional scales (Ayup-Zouain, 2006; Mahiques et al., 2008; Govin et al., 2012). To develop new sedimentary models, it is necessary to describe and understand major geomorphological features.

In the SAM, the Uruguayan continental slope (34–36°S) is located in the transition zone between the STSF and BMC (Franco-Fraguas et al., 2014) and in front of the RdlP mouth is bathed by the southernmost (summer) distribution of the RdlP buoyant plume (Piola et al., 2005; Möller Jr. et al., 2008; de Mello et al., 2014). Hence, it appears to be a key region in terms of regional circulation, especially for understanding the oceanographic control on slope sedimentary processes. In the region, these processes have only recently been the focus of sea floor research that has confirmed its interesting setting.

Using high spatial resolution and data obtained in situ, Franco-Fraguas et al. (2014) described the general morphological setting and stress in the surface sedimentological pattern of the Uruguayan slope. Based on oceanographic data, those authors found that the area presents complex sedimentary processes imprinted in glacial and interglacial times and characterized by a highly heterogeneous surface sedimentary environment. This environment is controlled by both the modern hydrology and slope configuration.

In addition to a large submarine canyon system, the configuration includes a sharp northward change in slope configuration.

Using bathymetric data and 2D and 3D seismic reflection profiles, Hernández-Molina et al. (2015), recently provided a detailed description of the configuration of this margin, demonstrating that it includes an impressive array of erosive, depositional and mixed contouritic features that were formed mainly by the northward displacement of Antarctic water masses from the Eocene to the present. According to those authors, the contourite features present good prolongation with the SAM SDS and vanish in the study region in response to the action of bottom currents during the migration of the BMC in glacial times. This highlights the importance of this region for subsequent sedimentary and paleoceanographic reconstructions.

However, to contribute precise reconstructions, specific questions concerning modern sedimentation need to be resolved. What are the source rocks of these sediments? Does the RdlP influence the organic matter in the slope sediments? What is the elemental content of the slope sediments? How does modern sedimentation relate to the glacial contouritic configuration?

To fill this gap, the aim of this paper is to build a sound sedimentary model framework for increasingly demanded palaeoclimatological and palaeoceanographical reconstructions studies in this key area of the SAM by synthesizing and correlating current evidence for modern (Franco-Fraguas et al., 2014) and ancient sedimentation (i.e., see Hernández-Molina et al., 2015) and integrating new sediment proxies for the input of sediments of the dominant hydrological systems (MC, BC and RdlP), for the contributions of terrestrial versus marine organic matter and for the depositional environment.

## 2. Regional setting

The SAM shelf circulation is closely associated with large-scale oceanographic processes that are not fully understood (Matano et al., 2010). Moreover, the regional circulation system experiences a seasonal latitudinal shift in response to wind regimes (Piola et al., 2005; Piola et al., 2008; Möller Jr. et al., 2008; Schmid and Garzoli, 2009).

At the surface, the low-salinity RdlP plume is displaced northwards along the inner Uruguayan continental shelf during the austral winter, but it remains off the mouth of the RdlP and extends along the entire continental upper margin during the austral summer and El Niño events (Piola et al., 2000; Piola et al., 2005; Möller Jr. et al., 2008). On the continental shelf below the RdlP plume, the southward-flowing Subtropical Shelf Waters (STSW) and the northward-flowing Subantarctic Shelf Waters (SASW) converge at the Subtropical Shelf Front (the shelf extension of the BMC) (Piola et al., 2008). These water masses, which are diluted by the continental runoff of the Rio de la Plata and the Patos Lagoon, are presumably detached offshore within the STSF (Piola et al., 2000). The STSF appears to remain latitudinally stable throughout the year, and it extends between 32°S at a water column depth of 50 metres and 36°S over the shelf break (Piola et al., 2000; Möller Jr. et al., 2008).

In the open ocean and at the BMC, the BC separates from the continental margin and collides with the MC, whereas the water masses are displaced offshore and flow as part of the South Atlantic Subtropical Gyre (Schmid and Garzoli, 2009).

The BC is a baroclinic boundary current whose main core is concentrated at a water depth of up to 500 m, and it carries Tropical Water (TW; Emilson, 1961; Piola and Matano, 2001; Palma et al., 2008) at the surface (0-200 metres) and South Atlantic Central Water (SACW; Emilson, 1961; Thomsen, 1962) below the surface (200-500 metres). However, the flux of the BC could be greater if it included the flux at the depth of the re-circulated AAIW that flows in the same direction as a result of the recirculation in the Subtropical Gyre (Steele et al., 2009). For practical purposes, we will hereafter refer to the flux of the re-circulated AAIW as part of the BC. The MC is a strong barotropic boundary current that advects Subantarctic Water (SAW; Thomsen, 1962) at the surface and Atlantic Intermediate Water below the surface (AAIW; Tomczak and Godfrey, 1994). The BMC zone is located at an average of approximately 38°S and is displaced northwards (36°S) during the austral winter and southwards during the summer (40°S, Schmid and Garzoli, 2009).

The SAM is characterized by an extensive continental shelf that widens to the south. The shelf is dominated by a relict sand coverture that was deposited under littoral, barrier and estuarine environments and was reworked during several Plio-Pleistocene transgressive–regressive events (Urien et al., 1980a, b; Lantzsch et al., 2014). Based on mineralogy (Ayup-Zouain, 2006), Nd isotopes (Mahiques et al., 2008) and elemental ratios (Govin et al., 2012), the imprint of the BC on the continental shelf can be tracked up to 25°S, whereas Pampean-Patagonian sediments advected by the MC dominate further south. The major sinks for the fine sediments transported along the RdlP winter buoyant plume are the well-known mud belts that extend along the inner continental shelf (Urien, 1967; Urien and Ewing, 1974; Ayup-Zouain, 2006; Lantzsch et al., 2014) and have an influence up to the Brazilian margin (Mahiques et al., 2004). However, the imprint of the RdlP summer plume on the slope open waters is still unknown, although its influence has been suggested (Frenz et al., 2003) and even assumed in several articles. Several authors concur regarding the influence of pyroclastic and volcanic sediments of Pampean–Patagonian origin transported northwards by the Malvinas Current (Teruggi, 1954; Etchichury and Remiro, 1960; Etchichury and Remiro, 1963; Bozzano et al., 2011). According to those authors, the coarse fraction is dominated by lithic fragments, quartz and feldspar grains. Using enviromagnetic, major element, and grain size data, Razik et al., (2015) further identified contrasting sources for the shelf and slope of the Argentinean Pampean margin. These include Pampean coastal wave erosion and westerly winds (shelf sediments) as well as Andean lowstand river input (slope sediments).

On the continental slope, the well-developed Contourite Depositional System (CDS), which is influenced by the displacement of subantarctic water masses, characterizes the Argentinean continental margin (Hernández-Molina et al., 2009; Violante et al., 2010). This alongshore process manifests both in the subsurface (Hernández-Molina et al., 2009; Violante et al., 2010) and surface sedimentation (Frenz et al., 2003; Bozzano et al., 2011).

This contourite system extends along the Uruguayan continental margin and presents good continuity in several erosive (terraces) and depositional (drifts) features (Hernández-Molina et al., 2015). Other important processes occurring in the region (submarine landslides and gravitational sediment transport) were recently reported on the deep Uruguayan and Argentinean margin (Krastel et al., 2011; Ai et al., 2014; Hernández-Molina et al., 2015). Submarine canyon systems (SCSs) are also a distinctive feature of the region and were first reported by Lonardi and Ewing (1971) between 35° and 38°S. The northernmost SCSs, the Rio de la Plata canyon system, extend into the study area (Franco-Fraguas et al., 2014; Soto et al., 2015; Hernández-Molina et al., 2015).

## 3. Materials and Methods

The study area is located along the Uruguayan outer shelf and upper and middle slopes between latitudes of 34°38′ S and 36°30′ S and longitudes of 52°00′ W and 53°30′ W (approximately 5000 km$^2$, Fig. 1).

In the austral summer of 2010, a high-resolution, large-scale sampling study was performed onboard B/O Miguel Oliver during a joint research cruise held by the Dirección Nacional de Recursos Acuáticos (DINARA, Uruguay), the Secretaría General del Mar (SGM) and the Instituto Español de Oceanografía (IEO) (Spain).

Based on in situ oceanographic, morphological and sedimentological (surface sediments) data, Franco-Fraguas et al. (2014, hereafter F-F) presented an environmental characterization of the study region. Classifications of superficial sediment facies (after Shepard (1954)) defined by the sum of all their known characteristics and using organic matter ($CaCO_2$, $C_{org}$, and $N_t$) content were interpreted in light of the environmental context. Extended descriptions of the methodological methods are presented in Franco-Fraguas et al. (2014). Briefly, bottom surface sediments were collected using a giant ULSNER-type box corer (0.25 m$^2$). In this study, we used the same superficial sample set used by F-F, so that only the topmost centimetre of sediment from undisturbed box corers was analysed for geochemical content.

Hernández-Molina et al. (2015, thereafter H-M) described the detailed morphosedimentary context and discussed the sedimentary, oceanographic and paleoceanographic implications along the entire Uruguayan slope based on integrated oceanographic, bathymetric, MultiChannel 2D and 3D Seismic reflection profiles (MCS) and well data. The detailed methodology can be seen elsewhere (H-M).

Partly for practical purposes, we first revised and re-named the surface facies classification after F-F. We then 1) integrated the oceanographic information provided by F-F and H-M and 2) correlated the morphological evidence (F-F) and re-named surface facies with the location of the morphosedimentary features presented by H-M. This provided a sound framework for the study area and is presented in the result section together with a brief description of the interpretation of the presented data after F-F and H-M. This framework was used to characterize and interpret the geochemical distribution of the proxies. A deeper analysis of the correspondence between the modern (F-F) and ancient (H-M) sedimentary processes will be presented elsewhere.

Immediately after sampling, the samples were frozen and stored for analyses of the following variables: grain size, organic carbon ($C_{org}$) and total nitrogen ($N_t$), stable isotopes ($\delta^{13}C$ and $\delta^{15}N$), major (Si, Ti, Fe, Al, K, Mn, Ca, P, and Mg) and trace (Ba) elements, and neodymium isotopes (εNd). These analyses were performed on 36 samples, with the exception of the εNd isotopes, which were determined for eight samples (Supplementary material 1, Fig. 1).

The grain size analyses were performed using low-angle light scattering (LALLS; coupled with a Malvern Mastersizer 2000 analyser) after acidifying the samples to eliminate the $CaCO_3$.

The $C_{org}$, $N_t$, $\delta^{13}C_{(PDB,\ Pee\ Dee\ Belemnite)}$ and $\delta^{15}N_{(Air)}$ were determined at the Oceanographic Institute of the University of São Paulo, Brazil, using a Finnigan Delta V Plus coupled with a Costech Elemental Analyser. The reference materials used for the $\delta^{13}C$ analysis were IA-R001 (wheat flour standard, $\delta^{13}C_{v\text{-}PDB}$ = - 26.43 ‰), IAEA-CH-6 (sucrose, $\delta^{13}C_{vPDB}$ = - 10.43 ‰) and IA-R005 (beet sugar, $\delta^{13}C_{v\text{-}PDB}$= - 26.30 ‰). IAEA-CH-6 is an inter-laboratory comparison standard distributed by the International Atomic Energy Agency (IAEA). IA-R001 and IA-R006 are calibrated against and traceable to IAEA-CH-6. The reference materials used for the $\delta^{15}N$‰ analysis were IA-R001 (wheat flour standard, $\delta^{15}N_{Air}$ = +2.55 ‰), IA-R045 (ammonium sulfate, $\delta^{15}N_{Air}$= + 4.71 ‰) and IA-R046 (ammonium sulfate, $\delta^{15}N_{Air}$ = + 22.04 ‰). IA-R001, IA-R045 and IA-R046 are traceable to IAEA-N-1 (ammonium sulfate, $\delta^{15}N_{Air}$ = + 0.4 ‰), an inter-laboratory comparison standard distributed by the IAEA.

The major and trace element contents of the bulk sediment were analysed via X-ray fluorescence (XRF) on fused glass discs at the Institute of Geosciences of the University of São Paulo, Brazil, following the analytical procedures described in Mori et al. (1999). The detection limit was below 10 ppm for the minor elements. The loss was determined based on differences in weight, thereby allowing for the measurement of total values and, hence, quality control.

According to Mahiques et al. (2008), grain size has no significant influence on fine sediment (silts and clays) Nd signals along the South American margin. Hence, the neodymium isotopic analysis was applied to the bulk lithological fraction of the finest grain size composition (i.e., > 15% of clay (<0.002 µm)). However, Nd values can depend on grain size in the coarse sediment fraction (Revel et al., 1996; Innocent et al., 2000). Considering this and the fact that samples for Nd isotopes were not available for the northern upper slope, the signals of the element ratios registered in bulk sediment samples collected along the South American margin (Fe/K and Al/Si; Govin et al., 2012) were used to further evaluate the origins of the lithogenic sediments. The Nd isotopic analyses were performed using a Finnigan MAT 262 multi-collector mass spectrometer at the Geochronological Research Center of the University of São Paulo, Brazil (see Mahiques et al. (2008) for the analytical procedures).

The sand and mud (silt/clay) fractions were used for correlation with the minor and major element contents and for interrelations between these variables (PCA, Principal Component Analysis).

Distribution maps of single elements (Si, Ti, Fe, Al, K, Mn, Ca, P, Mg, and Ba) were generated based on spatial (natural neighbour) interpolation methods using the ArcGIS 9.3 geographic information system.

## 4. Results

The distribution of renamed superficial facies classification (Facies 1 to 5) is presented in Fig. 2. Table 1 summarizes the correspondence between the morphological data and surface facies after F-F, renamed surface facies (this paper) and geomorphological features after H-M. Because the single element content correlated with the local depositional facies, that correlation is also presented in Table 1.

### 4.1 Framework

F-F divided the study area into 1) three latitudinal sectors, namely the southern, central and northern regions, 2) three bathymetric regions, namely the outer shelf (down to ca. 180 m), upper slope (from 180 to 500 m, including the shallow regions from 180 to 250 m and the lower regions from 250 to 500 m) and middle slope (from 500 to 1000 m), and 3) intra-canyon versus canyon regions (Fig, 2). This division was used for further correlations.

#### 4.1.1 Integration of oceanographic information

The upper layer is dominated by the distribution of the RdlP buoyant plume during the austral summer and el Niño events (de Mello et al., 2014). The upper slope is bathed by the MC and STSF in the south and by the BC in the north (F-F, H-M). F-F identified that the middle slope is dominated by the AAIW. However, a more detailed analysis of hydrological data allowed the differentiation of fresh AAIW from re-circulated AAIW

(H-M). In general, re-circulated AAIW dominates the study area, whereas the influence of the fresh northward-flowing AAIW is southward and extends towards the north (up to 34°S) as a narrow band at ca. 500 m beyond the location of the Brazil/Malvinas Confluence.

### 4.1.2 Correlation between seafloor data

There is a close correspondence between the seafloor data. Four submarine canyons, which were presented by F-F from south to north as canyons D, C, B, and A (Fig. 2), are incised in the middle slope (D, C) and in the upper slope (B, A) (F-F) and correspond with the Piriápolis SCS, José Ignacio SCS, La Paloma SCS and Cabo Polonio Mega Slide and SCS registered by H-M. In the north, gullies (Fig. 2) correlate with the Punta del Diablo SCS.

A sharp northward decrease in the slope concavity and deepening of the continental slope registered in the central region (F-F) correlate with the disappearance of the main contouritic terraces (T1 and T2), changing sharply towards a progradational slope (H-M). These terraces were formed by the upper (T1) and lower (T2) limit of the fresh AAIW during glacial stages and represent the prolongation of the La Plata and Ewing terraces in the Argentinean CDS (H-M). Canyon A (Cabo Polonio Mega Slide and SCS) coincides with the disappearance of contouritic T2 (H-M).

Facies 1: The facies corresponds to “Sands” and is present in the outer shelf and shallow upper slope throughout the region and nearby submarine canyon heads. This facies reflect a re-worked shelf, off-shelf transport and canyon lag-deposits, respectively (F-F). In the shallow upper slope, this facies coincides with T0 as described by H-M. T0 is distributed throughout the study area and coincides with the upper depth range of the SACW.

Southward (in a contouritic slope); 1) Facies 2: “Sandy silts” (named as Sub-facies A in F-F) with high organic matter and silt content, a dominant feature in the southern lower upper slope, is distributed on contouritic T1. This depositional facies was interpreted as controlled by the MC and STSF and enhanced by the smooth slope characteristic of contouritic structures and by canyons incised in the middle slope (F-F); and 2) Facies 3: “Silty sands”, with high medium sand content, is characteristic of middle slope areas in the south-central region and is associated with a contouritic smooth erosional surface (transition between terraces T1 and T2) and upper region of T2. This facies was interpreted as an erosional deposit related to contouritic structures and the influence of fresh AAIW (F-F).

Northward (in a progradational slope); 1) Facies 4: “Silty sands”, a key feature of the northern upper slope, coincides with a smooth progradational slope. This facies was associated to the erosional action of the BC enhanced by the steep slope configuration and canyons incised in the upper slope (F-F); and 2) Facies 5: “Sandy silt” (named as Sub-facies A in F-F), with high clay content, is present in the northern portion of the middle slope and coincides with a steep progradational slope. This facies was interpreted as a depositional facies related to the decreased influence of the fresh northward flowing AAIW and vanishing of contouritic structures (F-F).

### 4.2 Surface geochemical content and distribution

The basic statistics for the analysed variables are summarized in the Supplementary material 2.

The sand and mud values ranged between 97.3% and 17.9% (mean 60.5%) and between 82.1% and 2.7% (mean 39.5%), respectively.

εNd values of approximately -2.2 (ranging from -1.7 to -2.6, Supplementary material 1) were recorded throughout the study area (Fig. 3). The values of the elemental ratios ranged between 1.34 and 2.11 (Fe/K ratio) and between 0.14 and 0.28 (Al/Si ratio) (Fig. 3).

The C/N values ranged between 2.3 and 10.4, □$^{13}$C varied between -20‰ and -22.9‰, and □$^{15}$N varied from 3‰ to 7.1‰ (Fig. 4).

The correlation coefficients between the textural variables and the minor and major elements are summarized in the Supplementary material 3. In the PCA, the elements with similar content patterns were clustered (Fig. 5, Supplementary material 4). The spatial distributions of the various elements in the study area are presented in Figs. 6 and 7 superimposed on the facies distribution herein renamed.

In the PCA results, Factors 1 to 3 explained 85.1% of the total variance. Factor 1 explained 49.39% of the total variance and was characterized by three groups of elements: Ti, Fe, Mn, Al and K (group I); P, Ca and Mg (group II); and Si (group III). Factor 2 explained 28.22% of the total variance and corresponded to Ba, K and Al (group IV).

The elements in group I (Ti, Fe, Mn, Al and K) were mutually correlated, with the exception of Al and K. All were positively correlated with the mud contents, albeit with high dispersion (Supplementary material 3). In the inter-canyon sediments, all those elements exhibited increasing content towards the north. Low values were registered in the south coinciding with facies 2 (upper slope) and the southern part of facies 3 (middle slope), and the higher values in the central/north coincided with facies 4 (upper slope) and northern part of facies 3 and facies 5 (middle slope) (Fig. 6, Table 1).

The elements in group II (Ca, P and Mg) were strongly correlated with the muddy sediments (Supplementary material 3). High contents of those elements were evident in facies 2 (Fig. 7, Table 1).

Silicon appears to be isolated in the PCA. This element was positively correlated with the sand content (Supplementary material 3), and high values were observed on facies 1 and, to a lesser extent, on the southern part of facies 3 (middle slope, Fig. 7, Table 1).

Ba, Al and K were grouped together (group IV), because they presented relatively high values in facies 1. Ba was positively correlated with Si and sand (Supplementary material 3), and they therefore shared a similar spatial distribution pattern (Fig. 7). Al and K shared the spatial pattern observed for the elements of group I (see above); however, they presented relatively high values in facies 1, primarily in the outer shelf and canyon heads (Fig. 6, Table 1).

## 5. Discussion

### 5.1 Interpretation of analysed variables

According to Mahiques et al. (2008), the Nd isotope values recorded here indicate that Andean volcanic rocks are the primary sediment source. Accordingly, the values of the elemental ratios are lower than those reflecting the Brazilian Precambrian granitic and metamorphic basements and the RdlP input and are comparable to the values that characterize the Argentinean margin (Govin et al., 2012) (Fig. 3). This indicates that these sediments are transported from the south within subantarctic water masses (eg. Ayup-Zouain, 2006; Mahiques et al., 2008; Razik et al., 2015).

However, the recorded values of the organic matter content are comparable to those of the surface sediments of the RdlP estuary and the adjacent continental shelf (Burone et al., 2013). The C/N values are similar to values representing estuarine–marine conditions, and the $\square^{13}C_{PDB}$ values are similar to estuarine values and are higher than those from strictly riverine stations (Fig. 4). Consequently, both proxies indicate a mixed marine contribution to the slope sediments. However, the $\square^{15}N$ values are generally higher than estuarine–marine values (Fig. 4), presumably indicating changes in the trophic level of the organic matter (Michener and Kaufman, 2007).

In general, the elements in Group I (Ti, Fe, Mn, Al and K) are associated with fine sediments as constituents of aluminosilicates as a result of scavenging in biogenic particles and/or absorption by clayey sediments (Murray and Leinen, 1996). Alternatively, they can be indicative of the mineralogy of coarse sediments (Govin et al., 2012). The correlation between the elements of Group I and mud indicates the occurrence of sedimentation as fine terrigenous particles (thereafter called terrigenous elements). Notwithstanding, the high dispersion of the regression residuals evidences its broad distribution in the area. However, the particular behaviour of Al and K further responds to coarse sedimentation (see below).

The relation between the elements of Group II (Ca, P and Mg) and muddy sediments suggests a biogenic composition (Wei et al., 2003) (thereafter called biogenic elements). The geographical coincidence between the high contents of these elements and high $CaCO_3$, $C_{org}$ and $N_t$ (F-F) corroborates the biogenic origin of these elements.

The elements of Group III (Si) and Group IV (Ba, Al and K) are geographically associated with the erosional environments (thereafter called erosional elements). Si can be derived from aluminosilicates, quartz grains and silicious plankton (diatoms and radiolarians). Although a biogenic source for the Si could occur along this region (Romero and Hensen, 2002), the low values of Si observed within the biogenic facies (group II) suggests that this Si source is relatively scarce. Conversely, the correlation with sandy sediments indicates that the high Si content mainly reflects a high quartz content.

In marine sediments, Ba is associated with both detritic and biogenic particles, and its predominant carriers are clays and barite, respectively (Gonneea and Paytan, 2006). Barium is one of the most widely used proxies for estimating productivity (Dymond et al., 1992; Paytan et al., 1996). Nevertheless, its use as a reliable indicator of variations in productivity over time has long been controversial (Calvert and Fontugne, 2001; Prakash Babu et al., 2002; Wei et al., 2003; Jacot Des Combes et al., 2005). Hence, regional Ba/Al ratios have been used primarily as indicators of marine vs. terrigenous influence (Burone et al., 2013). However, in sandy deposits, the Ba content generally increases with increasing Si content (Ure and Berrow, 1982). Therefore, considering the low values of Ba observed in the biogenic facies and its association with sand and Si, high values of Ba likely reflect mainly high terrigenous content. Accordingly, in addition to aluminosilicates, Al and K are also constituents of coarse feldspar grains. Quartz and feldspar grains have been reported as major constituents of the Pampean–Patagonian suite (Teruggi, 1954; Bozzano et al., 2011) but are common minerals in a huge number of different rocks.

## 5.2 Sedimentation model

In the Uruguayan margin from the long term influence of water masses from higher southern latitudes in combination with down-slope sedimentary processes have strongly controlled the overall margin morphology (Hernández-Molina et al., 2015). Palaeoceanographic shifts that included the arrival of Antarctic Intermediate Water along the margin during the middle/late Miocene epoch and further fluctuations of the

Brazil–Malvinas Confluence influenced subsequent glacial and interglacial stages (H-M).

In particular, the disappearance of main contouritic terraces T1 and T2 represents the imprint of the position of the BMC during large-scale geological glacial times (H-M). The correlation found between the distributions of surface deposits (F-F) and geomorphologic features and regions (H-M) indicates a strong morphological control on the deposition of the textural surface sediments (facies 1 to 5); in the south associated with the contouritic structures and in the north related to a progradational slope. This fine-tunes the previous findings of F-F, who found an important control of the general configuration of the margin and modern hydrological system on the modern sedimentation. The content of elements, however, presents a different distribution in relation to the distribution of textural facies, hence providing new information regarding modern sedimentation. The integrated analyses of these information together with results of provenance of particles and new modern hydrological data provided by H-M has allowed the proposal of an updated model that includes the dynamics related to the RdlP and BC, the main sedimentary processes that govern the modern sedimentation and its relation with past large-scale glacial sedimentation.

### 5.2.1 Sedimentation related to the RdlP and BC

Referring to previous hydrological data, one would expect to find that particles transported by the three main hydrological features (RdlP -whole area-, BC -central/north- and MC -south-) co-exist in the study area. Herein, the inferred unique sediment source indicates that the RdlP and BC had a negligible influence.

The re-packing of particles and effective sedimentation from buoyant plumes in oceanic basins depends on hydrological parameters that control the direction, speed, thickness and width of the plume and on the settling velocity, which is directly related to the sediment concentration and the turbulence on the edge of the plume (Hill et al., 2007). Hence, our results suggest that the features of the relatively thin (˜10 m, de Mello et al., 2014) summer RdlP buoyant plume (Möller Jr. et al., 2008), which spreads over a large area (Piola et al., 2005), precludes the effective sedimentation of particles on the continental slope. Moreover, the strong vertical gradient formed between the continental waters in the upper layer and the subsurface SASW (Möller Jr. et al., 2008) probably inhibits the deposition of river-derived inorganic matter, thus explaining the absence of any RdlP signature. This material could, in turn, be transported and deposited off-shore.

However, the RdlP influence is recorded in the mixed-marine organic matter deposited homogenously throughout the region. A similar settling mechanism governed the sedimentation of the inorganic and organic river-derived particles (Acha et al., 2004; Hill et al., 2007). Hence, the results indicate that the mixed-marine origin signature mainly reflects that the RdlP nutrient-rich coastal waters fertilize open waters and thereby influence the surface productivity at the slope extension of the STSF. Alternatively, some complex circulations (i.e., lateral advection; Hill et al., 2007) could allow sedimentation only from RdlP-derived organic matter.

The absence of a sediment signal from the north suggests 1) that sediments influenced by the BC (mainly central/north region) do not reflect the modern hydrology and instead represent sediments deposited when the hydrological system was located at some past northward position and/or that 2) the modern circulation does not allow its effective sedimentation.

In the upper slope, northwards, sedimentation (facies 4) is controlled by the strong action of the BC (F-F). Considering 1) the erosive nature of this facies, 2) the fact that the Uruguayan continental shelf is covered by relict reworked Pampean–Patagonian sediments (Ayup-Zouain, 2006) and important shelf export has been observed at this location (F-F), and 3) the shifts in the STSF in Holocene (Bender et al., 2013) and glacial times (H-M) implies that during modern times the BC virtually does not displace sediments towards these latitudes or this sedimentation is enabled by the BC polishing effect (Mahiques et al., 2011). Instead, it indicates that on the upper slope, the BC predominantly reworks ancient Pampean sediments.

In the middle slope, northwards, the depositional facies 5 represents modern sedimentation (ca. 400 yrs; unpublished data). Here, a narrow band of fresh AAIW dominates the 500 isobath, and re-circulated AAIW is dominant offshore (H-M). However, the latter water mass does not contact the seafloor at this latitude (H-M). Consequently, this circulation pattern may enable the sedimentation of particles transported by the re-circulated AAIW. Alternatively, it may reflect the low sediment transport capacity of this water mass. This is reasonable given that 1) the re-circulated AAIW has circulated along the Subtropical Gyre, 2) 2/3 of the AAIW that reaches the American margin circulates southward along the Brazilian margin, and 3) at subsurface levels, the mean transport of the BC between 30 and 35°S (5.2 ± 2.2 Sv) represents half of the transport of the MC (10.5±1.9 Sv) (Schmid and Garzoli, 2009).

### 5.2.2 Environmental control of the element distribution

The similar terrigenous contents observed between the upper and middle-slope sediments (in an otherwise depth-related pattern) in the study region suggest the across-slope redistribution of sediments towards the middle slope. This pattern, however, presents a latitudinally related variation that together with the distribution of biogenic and erosional elements suggests that contrasting sedimentary processes dominate the modern sedimentation. We will discuss these interpretations in the light of previous findings focused mainly in the southern and northern regions (F-F), also considering information on the distribution of AAIW (H-M). Sedimentation in the central region is discussed latter.

In the study area, although gravity-related processes have been previously observed, they were confined to off-shelf transport towards the shallow upper continental slope (Bender, 2012; Franco-Fraguas et al., 2014) and to the canyon heads (Franco-Fraguas et al., 2014), as indicated by high erosional (Si, Ba, Al and K) characteristic elements in sandy facies. According to Bender (2012), the off-shelf export could be related to the detachment of the STSF from the continental shelf.

In the north and associated with a progradational slope, the off-shelf export and erosion are stronger due to the action of the BC along with the relatively steep slope configuration (F-F). Below, in the middle slope, F-F argues that the fine sediments (facies 5) correspond to re-suspended sediments transported by along-slope processes from the south. This could be related to the recently observed narrow distribution of the fresh AAIW (H-M). However, this facies presents a dominant very fine sand mode (F-F) as well as a clay mode. It is difficult to imagine the occurrence of the along-slope transport and subsequent deposition of very fine sands ahead of the contourite deposits and extending across the Mega Slide Canyon (mean width 25 km (F-F); Fig. 2). Shelf and upper slope oceanographic processes (i.e., tides, storms and the BC) could promote, besides the off-shelf export of relict coastal deposits (F-F), sand spillover (Stow and Mayall, 2000) and/or sandy slumps (Shanmugam, 2000) towards the deep sea, thereby explaining the very fine sand mode mentioned above. These could, in turn, be related to the gullies observed there (F-F). The input of fine sediments could alternatively represent aeolian sediments transported across the continental shelf (Razik et al., 2015), promoted by the relatively low energetic environment that characterizes this facies.

In the south and related to a contouritic slope, the distributions of biogenic (upper slope, facies 2, T1) and erosional (middle slope, southern region of facies 3 and of the transition between T1 and T2) characteristic elements differentiate depth-related facies, helping to characterize their genesis in addition to explaining the observed latitudinal pattern in terrigenous elements. On the upper slope, the high biogenic and low terrigenous element content characterizes a highly productive facies that was interpreted to be controlled by the MC and STSF and enhanced by the relatively smooth slope (F-F). In highly productive marine regions, organic matter and carbonates can dilute single-element contents ("dilution effects"; Govin et al., 2012). According to de Mello et al. (2014), the average primary production observed in this region (i.e., 1362 g cm$^{-2}$ year$^{-1}$) is typical of highly productive areas. Accordingly, the organic carbon values recorded in this facies (up to 7%, Franco-Fraguas et al., 2014) are comparable to those recorded in upwelling regions (Mollenhauer et al., 2004). Hence, dilution effects may possibly explain the low values of terrigenous elements recorded in the south. On the middle slope, the relatively high erosional element content (Si and Ba) and low terrigenous content coincides with the modern distribution of fresh AAIW (H-M). Hence, the erosion of fine terrigenous elements could possibly explain the observed terrigenous elemental gradient.

### 5.3 Paleoceanographic implications

The latitudinal-related distribution of elements is in line with the interpretation of latitudinal-related processes as evidenced by the distribution of geomorphological features and superficial textural facies. However, this evidence indicates a clear latitudinal difference between the southern/central (contouritic) and northern (progradational) sedimentation (i.e., glacial sedimentation, H-M). In addition, the element contents registered here differentiate the southern from the central-northern regions, including a contrasting sedimentation pattern along T2. Taking into account that this distribution coincides with the modern hydrological distribution (H-M) suggests 1) that the geochemical sedimentation in the central zone is closest to the pattern of sedimentation that characterizes the northern region (across slope processes) and 2) that the sedimentary processes have shifted southward with respect to their glacial distribution. Therefore, this provides potential evidence of the shift of the BMC during the present interglacial time.

## 6. Conclusions

The integration of previous outstanding high-resolution evidence from both ancient and modern sedimentary processes has provided a sound framework to understand sedimentary processes along the Uruguayan margin. The analyses of geochemical proxies of the origin of lithogenic and organic matter particles, together with the contents of major and minor elements in surface sediments represent advancement in the knowledge of the regional sediment dynamics and their relationship with large-scale glacial sedimentation.

Results highlight a strong morphologic control on modern sedimentation; sedimentation is associated with contouritic terraces in the south, and related to a progradational slope in the north. However, geochemical proxies indicate that during the present interglacial the circulation regime precludes the input of lithogenic particles from the RdlP and BC, and that instead the southward retreat of the hydrological system in relation to glacial stages promotes the dominance of across-slope processes in otherwise contouritic deposits, restricting sedimentation associated with contouritic features to the south.

Studies that focus on past sedimentation will progress our understanding of the remarkable environment represented by the boundary between the contourite and progradational deposits. Considering the close relationship between the sedimentological and palaeoceanographic issues, the expanded sedimentation model presented here, including the geochemical imprint of the different sedimentary environments, will be important for developing more precise environmental reconstructions of this complex and highly productive region.

## Acknowledgements

This work was part of PFF's PhD thesis. We would like to express our gratitude to the R/V Miguel Oliver crew. Financial support from the *Secretaría General del Mar* (SGM) and *Instituto Español de Oceanografía* (IEO) (Spain) as well as from the *Dirección Nacional de Recursos Acuáticos* (DINARA) (Uruguay) is acknowledged. PFF acknowledges the *Agencia Nacional de Innovación e Investigación* (ANII, Uruguay) and *Programa de Investigación de Ciencias Básicas* (PEDECIBA). We are grateful to all the staff of the *Laboratorio de Oceanografia* and *Laboratorio de Tecnología Pesquera and Bentos* (DINARA), especially to Lic. Yamandu Marin, Mr. Fabrizio Scarabino, Msc. Arianna Masello, Msc. Gastón Martínez, Msc. Sebastián Horta and Mr. Julio Chocca. Dr. Carlos Maria Urien is specially acknowledged for fruitful shared discussions that provided key insights for the improvement of this contribution. Juan Trucco is acknowledged for providing the artwork for the synthetic diagram. Suggestions from Javier Hernandez-Molina, an anonymous reviewer and the editor greatly improved this manuscript. This is contribution N.1 to the Grupo deI Investigación en Ciencia y Tecnología Marina (CINCYTEMA).

Table 1 Correspondence between the morphological data and surface facies, updated surface facies, geomorphological features/regions and relative content of the groups of elements. [1] after Franco-Fraguas et al. (2014), [2] this work, and [3] after Hernández-Molina et al. (2015). The contouritic terraces are located at ~250 m (T0), ~500 m (T1) and ~1200 m (T2) (Hernández-Molina et al., 2015).

| Bathymetry[1]/ Latitudinal sectors[1] | South | Central | North |
|---|---|---|---|
| Vertical profile[1] | Smooth slope | Smooth slope | Concave, deep and sharp slope |
| Outer shelf (up to 180 m) | Sand/facies 1/high Si, Ba | | Sand/facies 1/high Si, Ba |
| Shallow upper slope (180-250 m) | Sand[1]/facies 1[2]/T0[3]/high Si, Ba[2] | | Sand/facies 1/T0/high Si, Ba |
| Lower upper slope (250-500 m) | Sandy silt with high organic content/facies 2/T1/high Ca, P, Mg | Silty sand/high Ti, Fe, Mn, Al, K | Silty sand/facies 4/smooth progradational/high Ti, Fe, Mn, Al, K |
| Middle slope (500-1000 m) | Silty sand with high mediun sand content/facies 3/Erosional surface (transition between T1 and T2) and part of T2/relatively high Si and Ba | Silty sand with high mediun sand content/facies 3/Erosional surface (transition between T1 and T2) and part of T2 /high Ti, Fe, Mn, Al, K | Sandy silt with high clay content/facies 5/sharp progradational/high Ti, Fe, Mn, Al, K |

**Figure Captions**

Figure 1. Regional circulation on the Southwestern Atlantic continental shelf and slope (re-drawn from Matano et al. 2010); *SASW*: Subantarctic Shelf Water; *STSF*: Subtropical Shelf Front; *BMC*: Brazil–Malvinas Confluence and location of the study area. Multibeam bathymetry and superficial sediment facies (based on the scheme of Shepard 1954) after Franco-Fraguas et al. (2014) showing the superficial element sample stations and Nd isotope sample stations used in this study.

Figure 2. Distribution of the updated superficial sediment facies superimposed on the multibeam bathymetry showing the latitudinal regions and canyons discussed in Franco-Fraguas et al. (2014). Bathymetrical regions described in section 4.1 after Franco-Fraguas et al. (2014) are shown with isobaths (250, 500, and 1000). Outer shelf and shallow upper slope (180-250 m), lower upper slope (250-500 m) and middle slope (500-1000 m).

Figure 3 (a) Nd and (b) Ln(Al/Si) and Ln(Fe/K) for sediments from the present study and from the three main sedimentary domains within the SAM: Argentinean, RdlP and Brazilian sediments (the latter data were obtained from Mahiques et al. (2008) -Nd- and Govin et al. (2012) -elemental ratios-). Note that the Al/Si and Fe/K ratios were Ln transformed for comparison with the Govin et al. (2012) dataset, the values of which are comparable to those of the Argentinean sediments. Fe/K values are not available for the Argentinean margin.

Figure 4 (a) C/N vs. □$^{15}$N and (b) □$^{13}$C vs. □$^{15}$N plots for sediments from the present study area and from the Rio de la Plata (the latter data extracted from Burone et al., 2013).

Figure 5 PCA plot of factor 1 vs. factor 2 depicting the interrelations between the minor and major elements and the grain size (sand and silt-clay), with the groups of variables indicated.

Figure 6 Distributions of the (a) Ti, (b) Fe, (c) Mn, (d) Al and (e) K contents (%) superimposed on the multibeam bathymetry after Franco-Fraguas et al (2014) and updated superficial sediment facies (cf. Fig. 2 for the colour coding).

Figure 7 Distributions of the (a) Ca, (b) P, (c) Mg, (d) Si and (e) Ba contents (units in % except for Ba, which is presented in mg/kg) superimposed on the multibeam bathymetry after Franco-Fraguas et al (2014) and updated superficial sediment facies (cf. Fig. 2 for the colour coding).

**References**

Acha, E.M., Mianzanb, H.W., Guerreroa, R.A., Faveroa, M., Bavab, J., 2004. Marine fronts at the continental shelves of austral South America Physical and ecological processes. Journal of Marine Systems 44, 83-105.

Ai, F., Strasser, M., Preu, B., Hanebuth, T.J.J., Krastel, S., Kopf, A., 2014. New constraints on oceanographic vs. seismic control on submarine landslide initiation: a geotechnical approach off Uruguay and northern Argentina. Geo-Marine Letters 34, 399-417.

Ayup-Zouain, R.N., 2006. Evolución paleogeografica y dispersión de los sedimentos del Rio de la Plata, in: Menafra, R., Rodriguez-Gallego, L., Scarabino, F., Conde, D. (Eds.), Bases para la conservación y el manejo de la costa uruguaya. Vida Silvestre, Montevideo, p. 668.

Bender, V.B., 2012. From shelf dynamics to shelf export: evidences from sedimetologic and paleoceanographyc slope record., Doctorate theses presented to Uuroprox. University of Bremen, Germany.

Bender, V.B., Hanebuth, T.J.J., Chiessi, C.M., 2013. Holocene shifts of the Subtropical Shelf Front off southeastern South America controlled by high and low latitude atmospheric forcings. Paleoceanography 28, 481–490.

Bozzano, G., Violante, R.A., Cerredo, M.E., 2011. Middle slope contourite deposits and associated sedimentary facies off NE Argentina. Geo-Marine Letters 31, 495-507.

Burone, L., Ortega, L., Franco-Fraguas, P., Mahiques, M., García-Rodríguez, F., Venturini, N., Marin, Y., Brugnoli, E., Nagai, R., Muniz, P., Bícego, M., Figueiras, R., Salaroli, A., 2013. A multiproxy study along the transition between the Río de la Plata and the adjacent Southwestern Atlantic inner Shelf to assess the sediment footprint of river vs. marine influence. Continental Shelf Research 55, 141–154.

Calvert, S.E., Fontugne, M.R., 2001. On the Late Pleistocene–Holocene sapropel record of climatic and oceanographic variability in the eastern Mediterranean. Paleoceanography 16, 78–94.

de Mello, C., Burone, L., Ortega, L., Franco-Fraguas, P., Lahuerta, N., Mahiques, M., Marin, Y., 2014. Benthic foraminiferal distributions on the Uruguayan continental margin (South-western Atlantic) and controlling environmental factors. Continental Shelf Research 9, 120–133.

DePaolo, D.J., 1988. Neodymium Isotope Geochemistry. An Introduction, Berlin.

Dymond, J.R., Suess, F., Lyle, M., 1992. Barium in deep-sea sediment: a geochemical proxy for paleoproductivity. Paleoceanography 7, 163–181.

Emilson, I., 1961. The shelf and coastal waters off southern Brazil. Boletim do Instituto Oceanográfico da Universidade de São Paulo 11, 101–112.

Etchichury, M.C., Remiro, J., 1963. La corriente de Malvinas y los sedimentos pampeano–patagónicos. Rev Museo Argentino Bernardino Rivadavia. Cs. Geológicas I.

Etchichury, M.C., Remiro, J.R., 1960. Muestras de fondo de la plataforma continental comprendida entre los paralelos 34° y 36°30 de latitud sur y los meridianos 53°10 y 56°30 de longitud oeste VI Rev Museo Arg Ciencia Nat Bernardino Rivadavia 4, 1–70.

Faganeli, J., Pezdic, J., Ogorelec, B., Misic, M., Najdek, M., 1994. The origin of sedimentary organic matter in the Adriatic. Continental Shelf Research 14, 365-384.

Framiñan, M.B., Brown, O.B., 1996. Study of the Río de la Plata turbidity front Part I: Spatial and temporal distribution. Continental Shelf Research 16, 1259-1282.

Franco-Fraguas, P., Burone, L., Mahiques, M., Ortega, L., Urien, C., Muñoz, A., López, G., Marin, Y., Carranza, A., Lahuerta, N., de Mello, C., 2014. Hydrodynamic and geomorphological controls on surface sedimentation at the Subtropical Shelf Front / Brazil–Malvinas Confluence transition off Uruguay (Southwestern Atlantic Continental Margin). Marine Geology 349, 24–36.

Frenz, M., Höppner, R., Stuut, J.B.W., Wagner, T., Henrich, R., 2003. Surface sediment bulk geochemistry and grain-size composition related to the oceanic circulation along the South American continental margin in the Southwest Atlantic, in: Wefer, G., Mulitza, S., Ratmeyer, V. (Eds.), The South Atlantic in the Late Quaternary: reconstruction of material budgets and current systems. Springer-Verlag Berlin Heidelberg New York Tokyo, pp. 347-373

Gonneea, M.E., Paytan, A., 2006. Phase associations of barium in marine sediments. Marine Chemistry 100, 124 – 135.

Govin, A., Holzwarth, U., Heslop, D., Keeling, L.F., Zabel, M., Mulitza, S., Collins, J.A., Chiessi, C.M., 2012. Distribution of major elements in Atlantic surface sediments (36°N–49°S): Imprint of terrigenous input and continental weathering. Geochemistry Geophysics Geosystems 13, Q01013.

Hernández-Molina, F.J., Paterlini, M., Violante, R., Marshall, P., de Isasi, M., Somoza, L., Rebesco, M., 2009. Contourite depositional system on the Argentine Slope: An exceptional record of the influence of Antarctic water masses. Geology 37, 507-510.

Hernández-Molina, F.J., Soto, M., Piola, A.R., Tomasini, J., B., P., Thompson, P., Badalini, G., Creaser, A., Violante, R.A., Morales, E., Paterlini, M., De Santa Ana, H., 2015. A contourite depositional system along the Uruguayan continental margin: Sedimentary, oceanographic and paleoceanographic implicat.. Marine Geology, DOI: 10.1016/j.margeo.2015.1010.1008.

Hill, P.S., Fox, J.M., Crockett, J.S., Curran, K.J., Friedrichs, C.T., Geyer, W.R., Milligan, T.G., Ogston, A.S., Puig, P., Scully, M.E., Traykovski, P.A., Wheatcroft, R.A., 2007. Sediment delivery to the seabed on continental margins, in: Nittrouer, C.A., Austin, J.A., Field, M.E., Kravitz, J.H., Syvitski, J.P.M., Wiberg, P.L. (Eds.), Continental Margin Sedimentation: From Sediment Transport to Sequence Stratigraphy. Blackwell Publishing Ltd International Association of Sedimentologists.

Innocent, C., Fagel, N., Hillaire-Marcel, C., 2000. Sm–Nd isotope systematics in deep-sea sediments: clay-size versus coarser fractions. Marine Geology 168, 79-87.

Jacot Des Combes, H., Caulet, J.P., Tribovillard, N.P., 2005. Monitoring the variations of the Socotra upwelling system during the last 250 kyr: a biogenic and geochemical approach. Palaeogeography, Palaeoclimatology, Palaeoecology 223, 243–259.

Krastel, S., Wefer, G., Hanebuth, T.J.J., Antobreh, A.A., Freudenthal, T., Preu, B., Schwenk, T., Strasser, M., Violante, R., Winkelmann, D., 2011. Sediment dynamics and geohazards off Uruguay and the de la Plata River region (northern Argentina and Uruguay) M78/3 shipboard scientific party. Geo-Marine Letters 31, 271-283.

Lantzsch, H., Hanebuth, T.J.J., Chiessi, C.M., Schwenk, T., Violante, R.A., 2014. The high-supply, current-dominated continental margin of southeastern South America during the late Quaternary. Quaternary Research 81, 339–354.

Lim, D.I., Jung, H.S., Choi, J.Y., Yang, S., Ahn, K.S., 2006. Geochemical compositions of river and shelf sediments in the Yellow Sea: Grain-size normalization and sediment provenance. Continental Shelf Research 26, 15–24.

Lonardi, A.G., Ewing, M., 1971. Sediment transport and distribution in the Argentine Basin. 4. Bathymetry of the continental margin. Argentine Basin and other related provinces. Canyons and sources of sediments, Physics and chemistry of the earth. Pergamon Press, Oxford, pp. 79-121.

Mahiques, M.M., Gaeta Tassinari, C.C., Marcolini, S., Violante, R.A., Lopes Figueira, R.C., Almeida da Silveira, I.C., Burone, L., Sousa, S.H.M., 2008. Nd and Pb isotopes signatures on the southeastern southamerica upper margin: implication for sediment transport and source rocks. Marine Geology 250, 51-63.

Mahiques, M.M., Mishima, Y., Rodrigues, M., 1999. Characteristics of the sedimentary organic matter on the inner and middle continental shelf between Guanabara Bay and Sao Francisco do Sul, Southeastern Brazilian Margin. Continental Shelf Research 18, 775-798.

Mahiques, M.M., Sousa, S.H., Burone, L., Nagai, R., Almeida da Silveira, I.C., Lopes Figueira, R.C., Soutelino, R.G., Ponsoni, L., Klein, D.A., 2011. Radiocarbon geochronology of the sediments of the São Paulo Bight (southern Brazilian upper margin). Analis da Academia Brasileira de Ciencias 83, 817-834.

Mahiques, M.M., Tessler, M.G., Ciotti, A.M., da Silveira, C.A., Sousa, S.H.M., Figueira, R.C.L., Tassinari, C.C.G., Furtado, V.V., Passos, R.F., 2004. Hydrodinamically driven patterns of recent sedimentation in the shelf and upper slope off Southeast Brazil. Continental Shelf Research 24, 1685-1697.

Martin, J.-M., Meybeck, M., 1979 Elemental mass-balance of material carried by major world rivers. Marine Chemistry 7, 173-206.

Matano, R.P., Palma, E.D., Piola, A.R., 2010. The influence of the Brazil and Malvinas Currents on the Southwestern Atlantic Shelf circulation. Ocean Science 6, 983-995.

Meyers, P.A., 1997. Organic geochemical proxies of paleoceanographic, paleolimnologic and paleoclimatic procceses. Organic Geochemistry 27, 213–250.

Michener, R.H., Kaufman, L.S., 2007. Stable Isotope Ratios as Tracers in Marine Food Webs: An Update, in: Lajtha, K., Michener, R.H. (Eds.), Stable

Isotopes in Ecology and Environmental Science. Second Edition. Blackwell Publishing Ltd. , pp. 238-278.

Mollenhauer, G., Schneider, R.R., Jennerjahn, T., Müller, P.J., Wefer, G., 2004. Organic carbon accumulation in the south atlantic ocean: its modern mid-Holocene and last glacial distribution. Global and Planetary Change 40, 249-266.

Möller Jr., O.O., Piola, A.R., Freitas, A.C., Campos, E.J.D., 2008. The effects of river discharge and seasonal winds on the shelf off southeastern South America. Continental Shelf Research 28, 1607– 1624.

Mori, P.E., Reeves, S.H., Correia, C.T., Haukka, M., 1999. Development of a fused glass disc XRF facility and comparison with the pressed powder pellet thechnique at Instituto de Geociências, São Paulo University. Revista Brasileira de Geociências 29, 441-446.

Müller, P.J., Suess, E., 1979. Productivity, sedimentation rate, and sedimentary organic matter in the oceans. Organic matter preservation. Deep-Sea Research Part A. Oceanographic Research Papers 26, 1347-1362.

Murray, R.W., Leinen, M., 1996. Scavenged excess aluminum and its relationship to bulk titanium in biogenic sediment from the central equatorial Pacific Ocean. Geochimica et Cosmochimica Acta 60, 3869-3878.

Murray, R.W., Leinen, M., Murray, D.W., Mix, A.C., Knowlto, C.W., 1995. Terrigenous Fe input and biogenic sedimentation in the glacial and interglacial equatorial Pacific Ocean. Global Geochemical Cycles 9, 667-684.

Olson, D.B., Podestá, G.P., Evans, R.H., Brown, O.B., 1988. Temporal variations in the separation of Brazil and Malvinas Currents. Deep Sea Research II 35, 1971-1990.

Palma, E.D., Matano, R.P., A.R., P., 2008. A numerical study of the Southwestern Atlantic Shelf circulation: Stratified ocean response to local and offshore forcing. Journal of Geophysical Research 113, 1–22.

Paytan, A., Kastner, M., Chavez, F.P., 1996. Glacial to interglacial fluctuations in productivity in the equatorial Pacific as indicated by marine barite. Science 274, 1355–1357.

Piola, A.R., Campos, E.J.D., Möller, J.O., Charo, M., Martinez, C., 2000. Subtropical shelf front off Eastern South America. Journal of Geophysical Research 105, 6565-6578.

Piola, A.R., Matano, R.P., 2001. The South Atlantic Western Boundary Currents Brazil/Falkland (Malvinas) Currents., in: Steele, J.M., Thorpe, S.A., Turekian, K.K. (Eds.), Encyclopedia of Ocean Sciences. Academic Press, London, UK, pp. 340-349.

Piola, A.R., Matano, R.P., Palma, E.D., Jr., O.M., Campos, E.J.D., 2005. The influence of the Plata River discharge on the western South Atlantic shelf. Geophysical Research Lettets 32, doi:10.1029/2004GL021638.

Piola, A.R., O.O., M.J., Guerrero, R.A., Campos, E.J.D., 2008. Variability of the Subtropical Shelf Front off eastern South America: winter 2003 and summer 2004. Continental Shelf Research 28, 1579-1588.

Prahl, F.G., Ertel, J.R., Goni, M.A., Sparrow, M.A., Eversmeyer, B., 1994. Terrestrial organic carbon contributions to sediments on the Washington margin. Geochimica et Cosmochimica Acta 58, 3035–3048.

Prakash Babu, C., Brumsack, H.J., Schnetger, B., Böttcher, M.E., 2002. Barium as a productivity proxy in continental margin sediments: a study from the eastern Arabian Seazs. Marine Geology 184, 189–206.

Razik, S., Govin, A., Chiessi, C.M., Dobeneck, T.v., 2015. Depositional provinces, dispersal, and origin of terrigenous sediments along the SE South American continental margin. Marine Geology 363, 261–272.

Revel, M., Cremer, M., Grousset, F.E., Labeyrie, L., 1996. Grain-size and Sr–Nd isotopes as tracer of paleo-bottom current strength, Northeast Atlantic Ocean. Marine Geology 131, 233-249.

Romero, O., Hensen, C., 2002. Oceanographic control of biogenic opal and diatoms in surface sediments of the Southwestern Atlantic. Marine Geology 186, 263-280.

Schmid, C., Garzoli, S.L., 2009. New observations of the spreading and variability of the Antarctic Intermediate Water in the Atlantic. Journal of Marine Research 67, 815–843.

Shanmugam, G., 2000. 50 years of the turbidite paradigm (1950´s-1990´s): deep-water processes and facies models-a critical perspective. Marine and Petroleum Geology 17, 174-231.

Shepard, F.P., 1954. Nomenclature based on sand-silt-clay ratios. Journal of Sediment Petrology 24, 151-158.

Shumilin, E.N., Carriquiry, J.D., Camacho-Ibar, V.F., Sapozhnikov, D., Kalmykov, S., Sanchez, A., Aguíñiga-García, S., Sapozhnikov, Y.A., 2002. Spatial and vertical distributions of elements in sediments of the Colorado River delta and Upper Gulf of California. Marine Chemistry 79, 113– 131.

Soto, M., Morales, E., Hernández-Molina, F.J., Veroslavsky, G., Tomasini, J., de Santa Ana, H., 2015. Procesos sedimentarios en el talud continental de Uruguay: una síntesis actualizada., in: Ciencias, D.-F.d. (Ed.), Montevideo.

Steele, J.H., Thorpe, S.A., Turekian, K.K., 2009. Ocean currents : a derivative of encyclopedia of ocean sciences. Academic Press, Amsterdam.

Stein, R., 1991. Accumulation of organic carbon in marine sediments. Results from the Deep Sea Drilling Project/Ocean Drilling Program. Lecture Notes in Earth Sciences 34, 217p.

Stow, D.A.V., Mayall, M., 2000. Deep-water sedimentary systems: New models for the 21st century. Marine and Petroleum Geology 17, 125-135.

Teruggi, M.E., 1954. El material volcánico-piroclástico en la sedimentación pampeana. AAS Revista 9, 184–191.

Thomsen, H., 1962. Masas de agua características del Océano Atlántico (parte Sudoeste). Buenos Aires: Servicio de Hidrografía Naval, Secretaría Marina, Publication H632, 1–27.

Tomczak, M., Godfrey, J.S., 1994. Regional Oceanography: An introduction. Pergamon Press.

Ure, A.M., Berrow, M.L., 1982. Environmental Chemistry, in: Bowen, H.J.M. (Ed.), The chemical constituents of soils. R. Soc. Chem., Burlington House, London, pp. 94-202.

Urien, C., 1967. Los sedimentos modernos del Río de la Plata exterior. Servicio de Hidrología Naval 4, 113-213.

Urien, C.M., Ewing, M., 1974. Recent sediments and environment of southern Brazil, Uruguay, Buenos Aires, and Rio Negro continental shelf, in: Burk, C.A., Drake, C.L. (Eds.), The Geology of Continental Margins. Springer, New York, N.Y., pp. 157-177.

Urien, C.M., Martins, L.R., Martins, I.R., 1980a. Evolução geológica do Quaternário do litoral atlântico uruguaio, plataforma continental e regiões vizinhas. Notas Técnicas, CECO/URFGS 3, 7-43.

Urien, C.M., Martins, L.R., Martins, I.R., 1980b. Modelos deposicionais na plataforma continental do Rio Grande do Sul (Brasil), Uruguai e Buenos Aires. Notas Técnicas, CECO/URFGS 3, 13-25.

Violante, R.A., Hernández-Molina, F.J., Paterlini, M., Bozzano, G., Krastel, S., Hanebuth, T., Preu, B., Laprida, C., 2010. Contouritic terraces on the Northern Argentina middle continental slope (southwestern Atlantic). Geo-temas 11, 183-184.

Wei, G., Liu, Y., Li, X., Chen, M., Wei, W., 2003. High-resolution elemental records from the South China Sea and their paleoproductivity implications. Paleoceanography 18, doi:10.1029/2002PA000826.

Weltje, G.J., Tjallingii, R., 2008. Calibration of XRF core scanners for quantitative geochemical logging of sediment cores: Theory and application. Earth and Planetary Science Letters 274, 423–438.

Yang, S., Youn, J., 2007. Geochemical compositions and provenance discrimination of the central south Yellow Sea sediments. Marine Geology 243, 229–241.

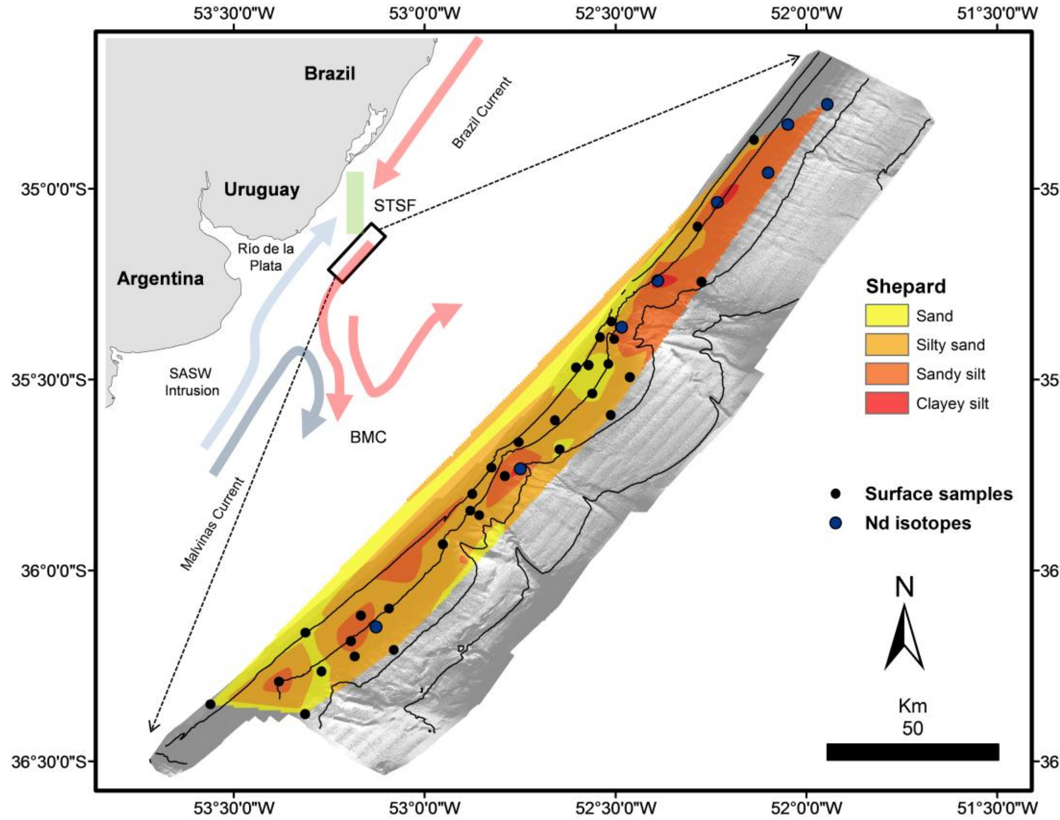
53°30'0"W
53°0'0"W
52°30'0"W
52°0'0"W
51°30'0"W
35°0'0"S
35°30'0"S
36°0'0"S
36°30'0"S
Brazil
Uruguay
Argentina
Rio de la Plata
Brazil Current
STSF
SASW Intrusion
BMC
Malvinas Current
Shepard
Sand
Silty sand
Sandy silt
Clayey silt
Surface samples
Nd isotopes
N
Km
50

Fig. 1

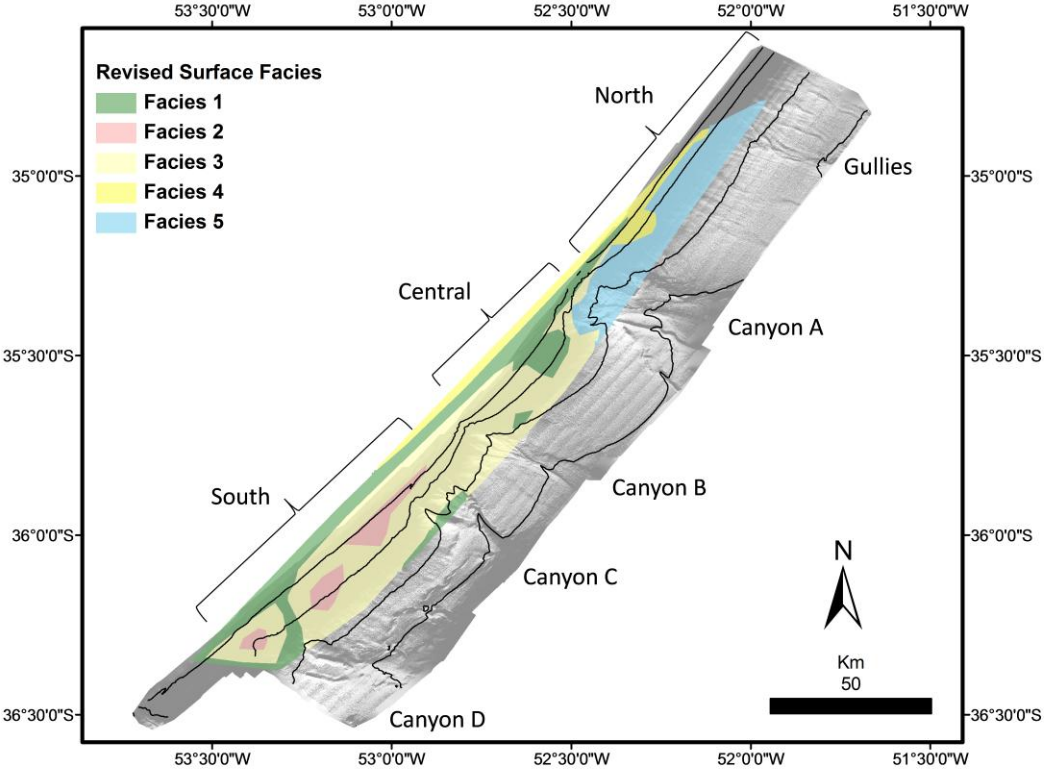
53°30'0"W
53°0'0"W
52°30'0"W
52°0'0"W
51°30'0"W
35°0'0"S
35°30'0"S
36°0'0"S
36°30'0"S
Revised Surface Facies
Facies 1
Facies 2
Facies 3
Facies 4
Facies 5
North
Central
South
Gullies
Canyon A
Canyon B
Canyon C
Canyon D
N
Km
50

Fig. 2

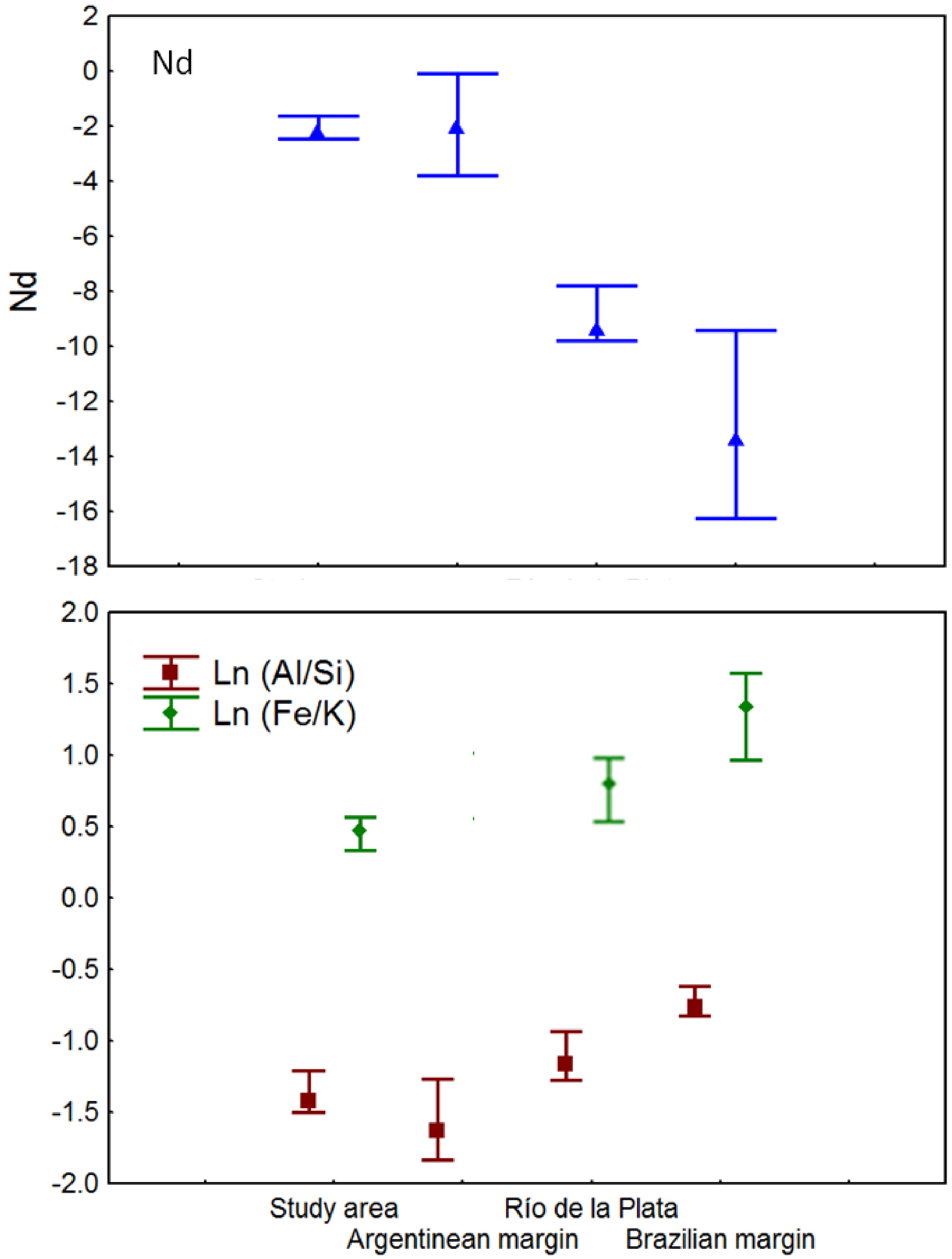
Nd
Nd
2
0
-2
-4
-6
-8
-10
-12
-14
-16
-18
Ln (Al/Si)
Ln (Fe/K)
2.0
1.5
1.0
0.5
0.0
-0.5
-1.0
-1.5
-2.0
Study area
Argentinean margin
Río de la Plata
Brazilian margin

Fig. 3

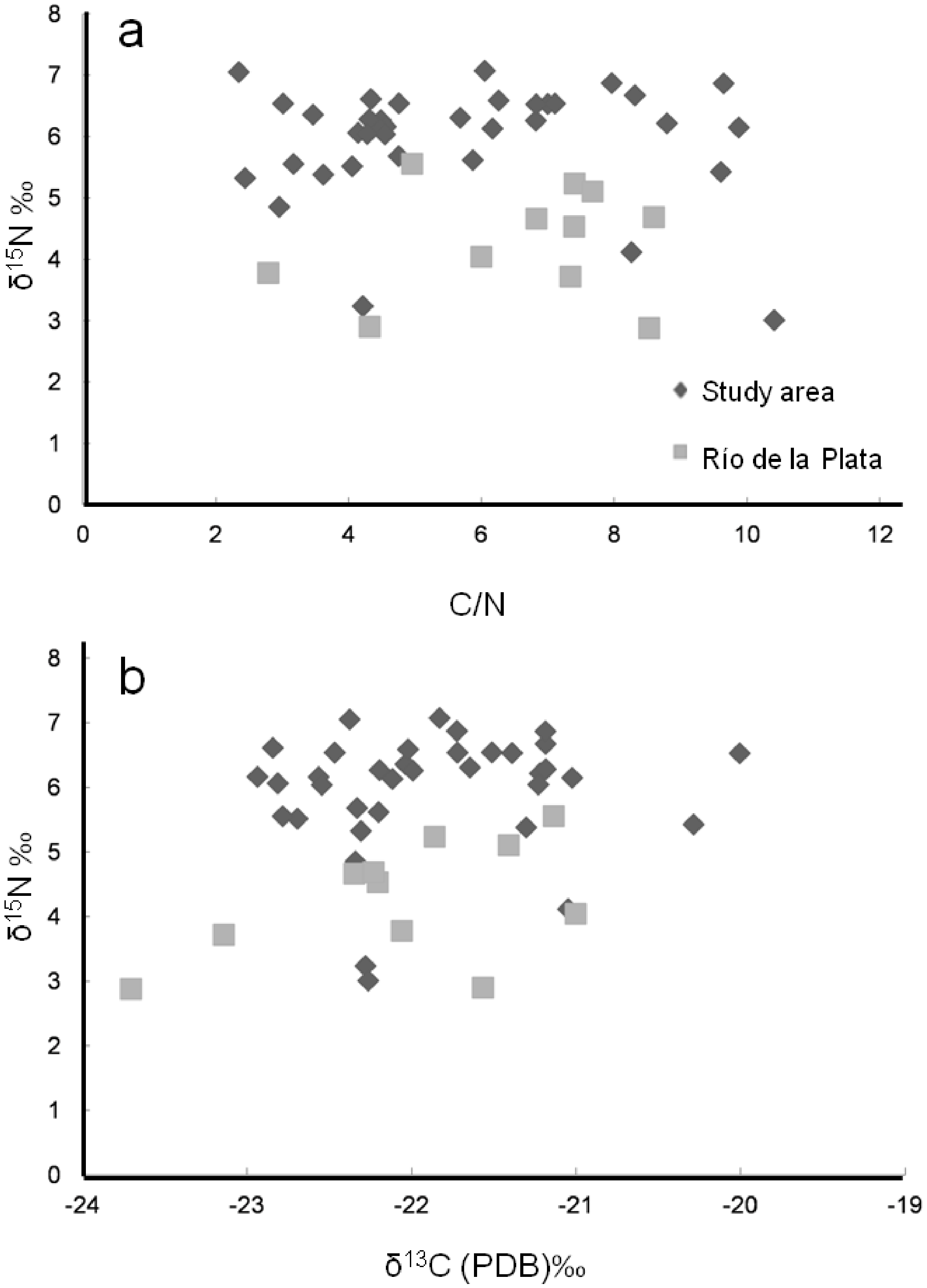
a
δ15N ‰
8
7
6
5
4
3
2
1
0
0
2
4
6
8
10
12
C/N
Study area
Río de la Plata
b
δ15N ‰
8
7
6
5
4
3
2
1
0
-24
-23
-22
-21
-20
-19
δ13C (PDB)‰

Fig. 4

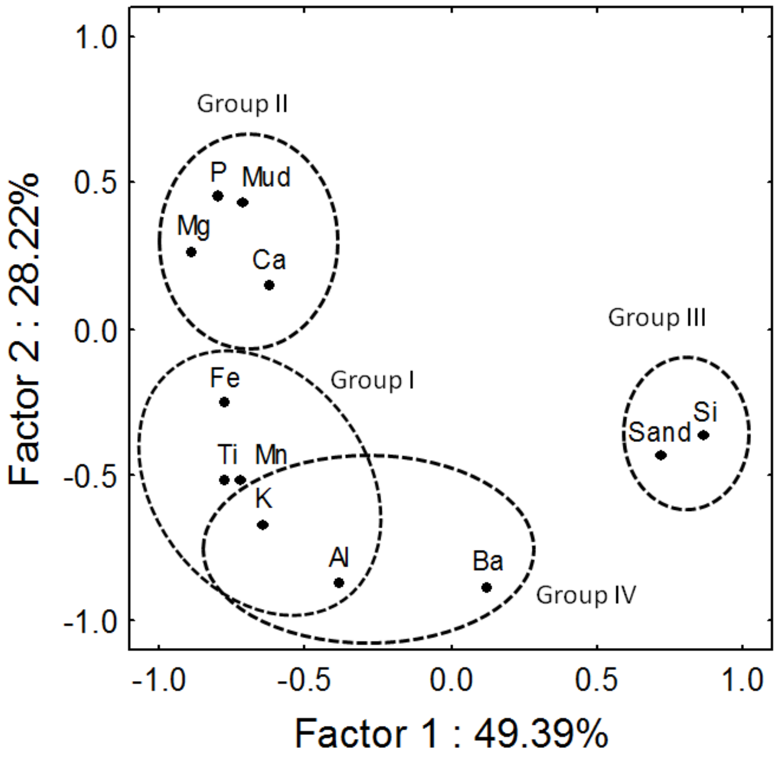
Factor 2 : 28.22%
Factor 1 : 49.39%
1.0
0.5
0.0
-0.5
-1.0
-1.0
-0.5
0.0
0.5
1.0
Group II
P
Mud
Mg
Ca
Group III
Fe
Group I
Si
Sand
Ti
Mn
K
Al
Ba
Group IV

Fig. 5

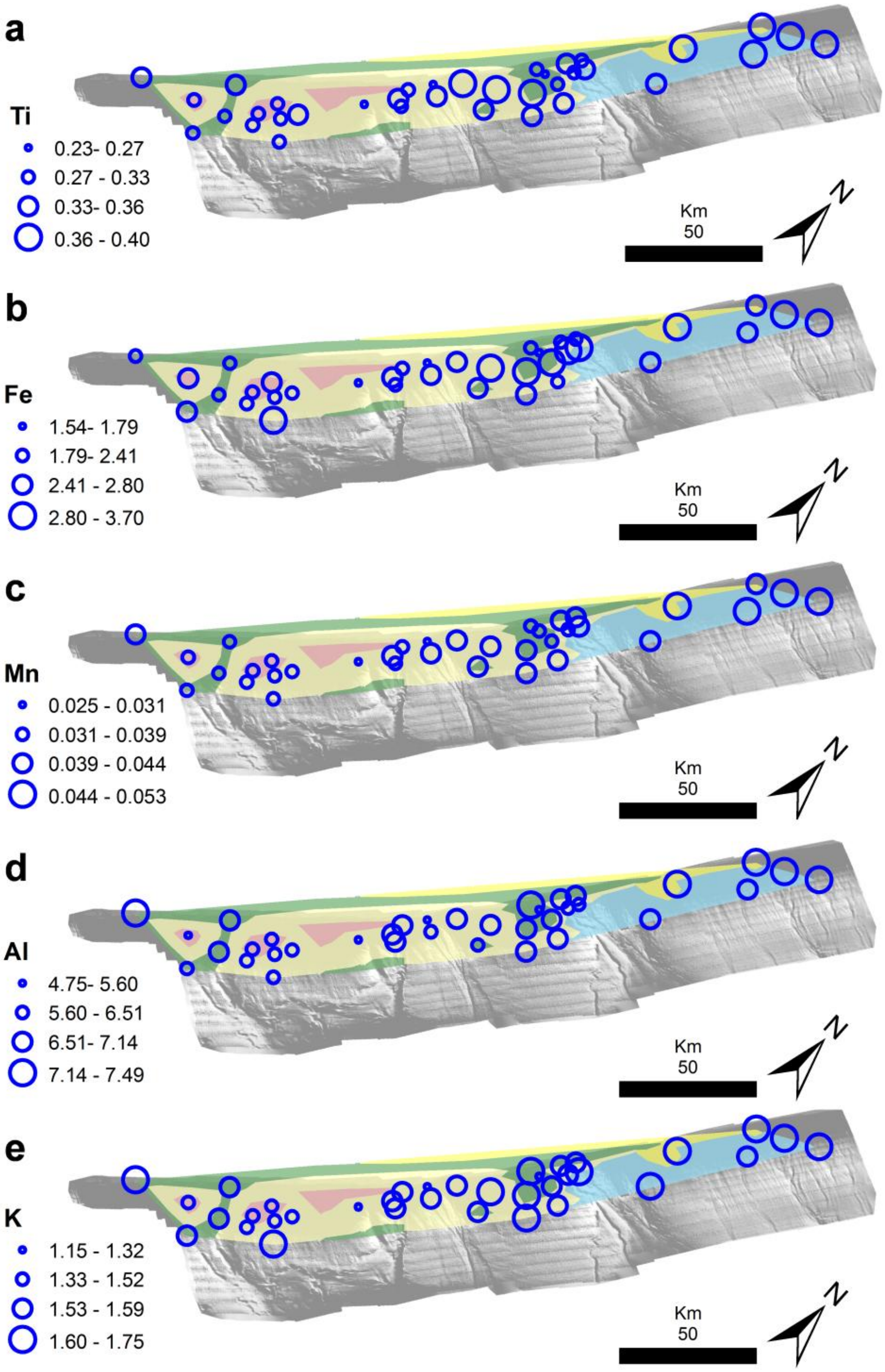
a
Ti
0.23- 0.27
0.27 - 0.33
0.33- 0.36
0.36 - 0.40
Km
50
N
b
Fe
1.54- 1.79
1.79- 2.41
2.41 - 2.80
2.80 - 3.70
Km
50
N
c
Mn
0.025 - 0.031
0.031 - 0.039
0.039 - 0.044
0.044 - 0.053
Km
50
N
d
Al
4.75- 5.60
5.60 - 6.51
6.51- 7.14
7.14 - 7.49
Km
50
N
e
K
1.15 - 1.32
1.33 - 1.52
1.53 - 1.59
1.60 - 1.75
Km
50
N

Fig. 6

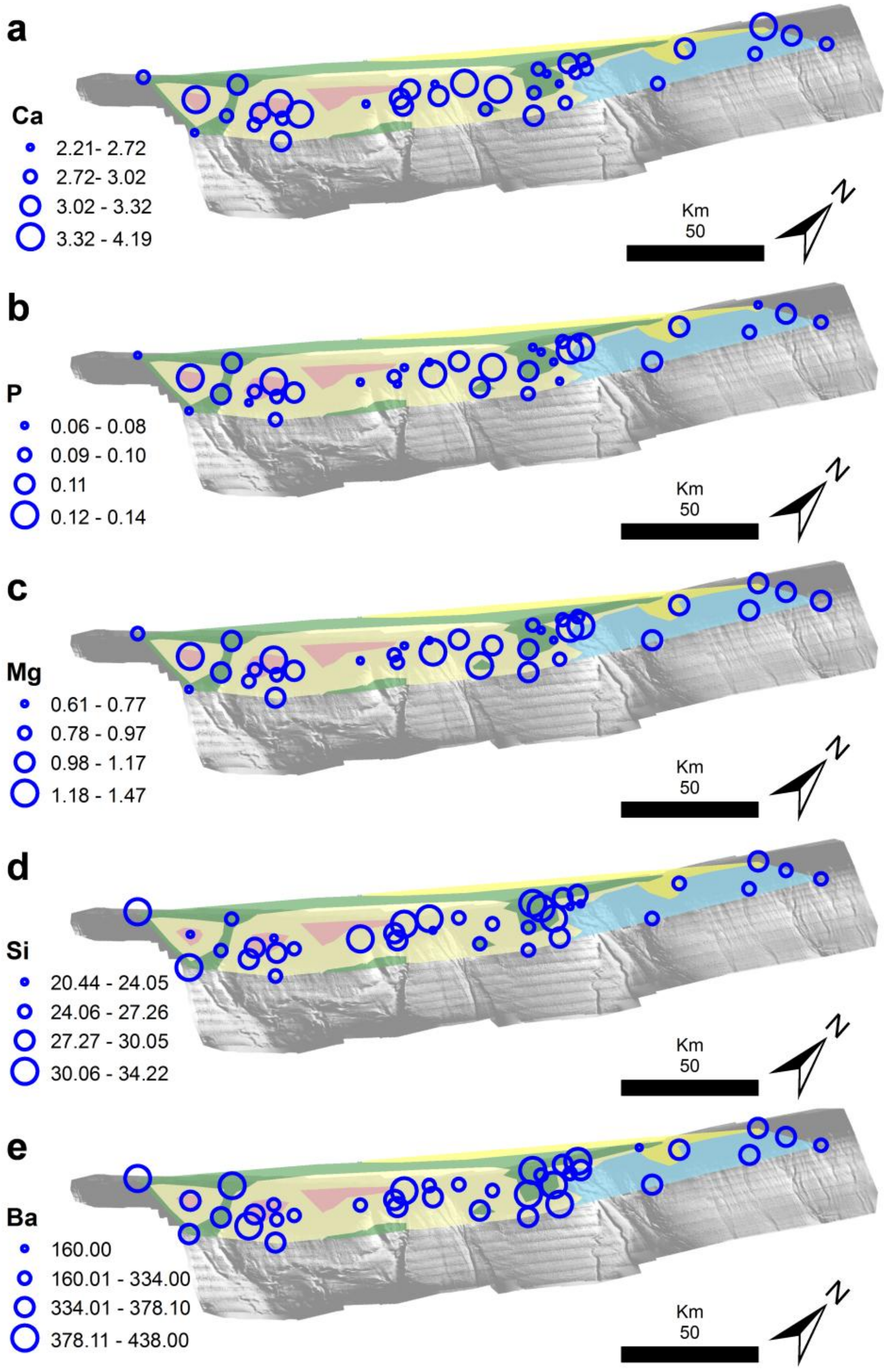
a
Ca
2.21- 2.72
2.72- 3.02
3.02 - 3.32
3.32 - 4.19
Km
50
N
b
P
0.06 - 0.08
0.09 - 0.10
0.11
0.12 - 0.14
Km
50
N
c
Mg
0.61 - 0.77
0.78 - 0.97
0.98 - 1.17
1.18 - 1.47
Km
50
N
d
Si
20.44 - 24.05
24.06 - 27.26
27.27 - 30.05
30.06 - 34.22
Km
50
N
e
Ba
160.00
160.01 - 334.00
334.01 - 378.10
378.11 - 438.00
Km
50
N

Fig. 7

**Highlights**

Integration of modern and ancient sedimentation data as sound framework
Results re-enforces the boundary between contourite and progradational configuration
New evidence on sediment provenance and sedimentary processes at the SAM
RdlP fertilizes open waters and low sediment transport of the BC is inferred
Evidences down slope transport toward the middle slope
A glacial/interglacial southward shift in sedimentation patterns is suggested